Universität des Saarlandes

Fachrichtung 6.1 – Mathematik

Preprint

Numerical solution of the Boltzmann equation on the uniform grid

I. Ibragimov & S. Rjasanow

Preprint No. 63

Saarbrücken 2002

Universität des Saarlandes

Fachrichtung 6.1 – Mathematik

Numerical solution of the Boltzmann equation on the uniform grid

I. Ibragimov & S. Rjasanow

Saarland University
Department of Mathematics
Postfach 15 11 50
D–66041 Saarbrücken
Germany
E-Mail: ilgis@num.uni-sb.de & rjasanow@num.uni-sb.de

submitted: June 17, 2002

Preprint No. 63

Saarbrücken 2002

Edited by
FR 6.1 – Mathematik
Im Stadtwald
D–66041 Saarbrücken
Germany

Fax: + 49 681 302 4443
e-mail: preprint@math.uni-sb.de
WWW: http://www.math.uni-sb.de/

Numerical solution of the Boltzmann equation on the uniform grid

I. Ibragimov & S. Rjasanow

Fachrichtung 6.1 - Mathematik

Universität des Saarlandes

66041 Saarbrücken

Germany

ilgis@num.uni-sb.de & rjasanow@num.uni-sb.de

June 17, 2002

Abstract

In the present paper a new numerical method for the Boltzmann equation is developed. The gain part of the collision integral is written in a form which allows its numerical computation on the uniform grid to be carried out efficiently. The amount of numerical work is shown to be of the order $O(n^6 \log(n))$ for the most general model of interaction and of the order $O(n^6)$ for the Variable Hard Spheres (VHS) interaction model, while the formal accuracy is of the order $O(n^{-2})$. Here n denotes the number of discretisation points in one direction of the velocity space. Some numerical examples for Maxwell pseudo-molecules and for the hard spheres model illustrate the accuracy and the efficiency of the method in comparison with DSMC computations.

AMS Subject Classification: 82C40, 82C80, 65R20
Keywords: Boltzmann equation, deterministic numerical method

1 Introduction

We consider the classical Boltzmann equation for a simple, dilute gas of particles [7]

$$f_t + (v, \mathrm{grad}_x f) = Q(f, f) \tag{1}$$

which describes the time evolution of the particle density $f(t,x,v)$

$$f \;:\; \mathbb{R}_+ \times \Omega \times \mathbb{R}^3 \to \mathbb{R}_+ .$$

Here $\mathbb{R}_+$ denotes the set of non-negative real numbers and $\Omega \subset \mathbb{R}^3$ is a domain in physical space. The right-hand side of the equation (1), known as the collision integral or the collision term, is of the form

$$Q(f,f)(v) = \int\limits_{\mathbb{R}^3} \int\limits_{S^2} B(v,w,e)\Big(f(v')f(w') - f(v)f(w)\Big)\, de\, dw\,. \tag{2}$$

Note that $Q(f,f)$ depends on t and x only as parameters, so we have omitted this dependence in (2) for conciseness. The following notations have been used in (2): $v, w \in \mathbb{R}^3$ are the pre-collision velocities, $e \in S^2 \subset \mathbb{R}^3$ is a unit vector, $v', w' \in \mathbb{R}^3$ are the post-collision velocities and $B(v,w,e)$ is the collision kernel. The operator $Q(f,f)$ represents the change of the distribution function $f(t,x,v)$ due to the binary collisions between particles. A single collision results in a change of the velocities of the colliding partners $v, w \;\to v', w'$ with

$$v' = \frac{1}{2}\Big(v + w + |u|\, e\Big),\;\; w' = \frac{1}{2}\Big(v + w - |u|\, e\Big)\,,$$

where $u = v - w$ denotes the relative velocity. The Boltzmann equation (1) is subjected to an initial condition

$$f(0,x,v) = f_0(x,v),\;\; x \in \Omega,\;\; v \in \mathbb{R}^3$$

and to the boundary conditions on $\Gamma = \partial\Omega$. The kernel $B(v,w,e)$ can be written as

$$B(v,w,e) = B(|u|,\mu) = |u|\sigma(|u|,\mu),\;\; \mu = \cos(\theta) = \frac{(u,e)}{|u|}\,.$$

The function $\sigma : \mathbb{R}_+ \times [-1,1] \to \mathbb{R}_+$ is the differential cross-section and θ is the scattering angle. Some special models for the kernel are as follows:

1. The **hard spheres model** is described by the kernel

$$B(|u|,\mu) = \frac{d^2}{4}|u|\,, \tag{3}$$

where d denotes the diameter of the particles.

2. The kernel

$$B(|u|,\mu) = |u|^{1-4/m} g_m(\mu)\,,\ m > 1 \tag{4}$$

corresponds to the **inverse power potential** of interaction. m denotes the order of the potential and g_m is a given function of the scattering angle only. The function g_m imposes a non-integrable singularity for $\theta \to 0$

$$g_m(\mu) = O\Big(\theta^{-\frac{m+2}{m}}\Big)\,.$$

Since the collisions with a small scattering angle lead to only small changes it is useful to cut off the function g_m in such a way that the condition $g_m \in \mathbb{L}_1([-1,1])$ is fulfilled [9]. This model of interaction is called **inverse power cut-off potential**. In this case the collision integral can be decomposed naturally

$$Q(f,f)(v) = Q_+(f,f)(v) - Q_-(f,f)(v)\,,$$

into the gain

$$Q_+(f,f)(v) = \int\limits_{\mathbb{R}^3}\int\limits_{S^2} B(|u|,\mu) f(v') f(w')\, de\, dw \tag{5}$$

and the loss part

$$Q_-(f,f)(v) = f(v) \int\limits_{\mathbb{R}^3} B_{tot}(|u|) f(w)\, dw\,. \tag{6}$$

In (6) $B_{tot}(|u|)$ denotes the following integral

$$B_{tot}(|u|) = \int\limits_{S^2} B(|u|,\mu)\, de\,. \tag{7}$$

3. The special case of $m = 4$ in (4) corresponds to the **Maxwell pseudo–molecules** with

$$B(|u|,\mu) = g_4(\mu)\,.$$

The collision kernel $B(|u|,\mu)$ here does not depend on the relative speed $|u|$.

4. The **Variable Hard Spheres model** [1] (VHS) has an isotropic cut-off kernel

$$B(|u|,\mu) = C_\lambda |u|^\lambda\,,\ -3 < \lambda \le 1. \tag{8}$$

The model includes, as particular cases, the hard spheres model for $\lambda = 1$ and a special case of the Maxwell pseudo–molecules with $\lambda = 0$.

All relevant physical values of the gas flow are computed as the first 13 moments of the distribution function or their combinations. These moments are:
the density

$$\varrho(t,x) = \int\limits_{\mathbb{R}^3} f(t,x,v)\,dv\,, \tag{9}$$

the momentum

$$m(t,x) = \int\limits_{\mathbb{R}^3} v\, f(t,x,v)\,dv\,, \tag{10}$$

the momentum flow

$$M(t,x) = \int\limits_{\mathbb{R}^3} vv^T\, f(t,x,v)\,dv\,, \tag{11}$$

and the energy flow

$$r(t,x) = \frac{1}{2}\int\limits_{\mathbb{R}^3} v|v|^2\, f(t,x,v)\,dv\,. \tag{12}$$

Note that the matrix $M(t,x)$ is symmetric and therefore defined by its upper triangle. Using these moments we define the bulk velocity

$$V(t,x) = \frac{m}{\varrho}, \tag{13}$$

the internal energy and the temperature

$$e(t,x) = \frac{1}{2\,\varrho}\left(\mathrm{tr}M - \varrho|V|^2\right),\ T(t,x) = \frac{2}{3R}e, \tag{14}$$

the pressure

$$p(t,x) = \varrho\, R\, T, \tag{15}$$

the stress tensor

$$P(t,x) = M - \varrho VV^T$$

and the heat flux vector

$$q(t,x) = r - \left(M + \left(\frac{1}{2}\mathrm{tr}M - \varrho|V|^2 \right) I \right) V \,.$$

Note that in the spatially homogeneous case $f = f(t,v)$ the following important conservation properties hold. The density

$$\varrho(t) = \int\limits_{\mathbb{R}^3} f(t,v)\, dv = \int\limits_{\mathbb{R}^3} f_0(v)\, dv = \varrho_0 \,, \tag{16}$$

the momentum

$$m(t) = \int\limits_{\mathbb{R}^3} v\, f(t,v)\, dv = \int\limits_{\mathbb{R}^3} v\, f_0(v)\, dv \tag{17}$$

and the trace of the momentum flow

$$\mathrm{tr}M(t) = \int\limits_{\mathbb{R}^3} |v|^2\, f(t,v)\, dv = \int\limits_{\mathbb{R}^3} |v|^2\, f_0(v)\, dv \tag{18}$$

remain constant during the relaxation. Thus, corresponding to (13), (14) and (15), the bulk velocity, the internal energy, the temperature and the pressure are conserved quantities

$$V(t) = V_0 \,,\ e(t) = e_0 \,,\ T(t) = T_0 \,,\ p(t) = p_0 \,.$$

Before we begin the description of our new numerical method, we shall discuss the results known from the literature. One of the first discrete versions of the Boltzmann equation was published by D. Goldstein, B. Sturtevant and J.E. Broadwell [8]. Many authors then published different ideas to lead to a discrete version of the Boltzmann collision operator [20], [12], [13], [14], [15], [16]. In [10] the authors studied the difference scheme for a mixture of gases. L. Pareschi and G. Russso [18], [19] considered deterministic spectral methods for the Boltzmann equation.
The main difficulty with the deterministic approximation of the Boltzmann collision integral besides its high dimensionality is the fact that any grid for the integration over the whole space $\mathbb{R}^3$ will not fit for the integration over the unit sphere S^2. Thus only $O(n)$ irregularly distributed integration

points belong to the unit sphere if n regular points in one direction are used for the approximation of the $\mathbb{R}^3$ integral. A. Bobylev, A. Palczewski and J. Schneider [3] considered this direct approximation of the Boltzmann collision integral and showed that the corresponding numerical method is consistent. The arithmetical work is $O(n^7)$ per time step and the formal accuracy is $O(n^{-1/2})$.

A. Bobylev and S. Rjasanow [4], [6] developed and tested a deterministic numerical method for the case of the Maxwell pseudo–molecules applying the Fast Fourier Transform (FFT) and using the explicit simplification of the Boltzmann equation for this model of interaction (see [2]). The arithmetical work is $O(n^4)$ per time step for the same low formal accuracy of $O(n^{-1/2})$. A similar method was considered by L. Pareschi and B. Perthame in [17]. Probably it is the fastest deterministic numerical method known but at the same time it is strongly restricted to the case of Maxwell pseudo–molecules. In the case of hard spheres A. Bobylev and S. Rjasanow [5] developed an algorithm where the integration over the unit sphere is completely separated from the integration over the whole space $\mathbb{R}^3$. The resulting scheme uses the possibility of fast evaluation of the generalised Radon and X-Ray transforms via FFT and requires $O(n^6 \log(n))$ per time step for the high formal accuracy of $O(n^{-2})$.

The paper is organised as follows. In Section 2 we show how to rewrite the gain part of the Boltzmann collision integral in a formally equivalent form which is convenient for the numerics for the most general model of interaction (4). In Section 3 we describe the uniform discretisation of the velocity space. The numerical algorithm for the Boltzmann equation with the general kernel will be formulated in Subsection 3.2. Then, in Subsection 3.3, we deal with the VHS model and construct a faster modification of the method described above. In Subsection 3.4 we discuss the discrete form of the conservation laws. The time discretisation is the topic of Subsection 3.5. In the fourth and final Section we present the results of some numerical tests. Here we use the analytically known time relaxation of the moments (9)-(12) for the Maxwell pseudo-molecules model for a careful check of the accuracy. Finally, a reference solution obtained by the DSMC method for the hard spheres model is compared with results obtained by the new method.

2 Transformation of the collision integral

The three-dimensional Fourier transform of the function $g(v)$ is defined as

$$\hat{g}(\xi) = \mathcal{F}_{v\to\xi}\Big[g(v)\Big](\xi) = \int\limits_{\mathbb{R}^3} g(v)\, e^{\imath(v,\,\xi)}\, dv\,. \tag{19}$$

Thus the function $g(v)$ can be represented as

$$g(v) = \mathcal{F}^{-1}_{\xi\to v}\Big[\hat{g}(\xi)\Big](v) = \frac{1}{(2\pi)^3}\int\limits_{\mathbb{R}^3} \hat{g}(\xi)\, e^{-\imath(v,\,\xi)} d\xi\,. \tag{20}$$

Lemma 1 *The gain part of the Boltzmann collision integral (2) can be written in the following form*

$$Q_+(f,f)(v) = \mathcal{F}_{y\to v}\Big[\int\limits_{\mathbb{R}^3} T(u,y)\mathcal{F}^{-1}_{z\to y}\Big[f(z-u)f(z+u)\Big](u,y)\,du\Big](v) \tag{21}$$

where the kernel $T(u,y)$ is defined as follows

$$T(u,y) = 8\int\limits_{S^2} B(2|u|,\mu)e^{-\imath|u|(y,\,e)}\,de\,. \tag{22}$$

Proof. Using the substitution $w = v - u\,,\ dw = du$ we rewrite the gain part of the Boltzmann collision integral (5) as follows

$$Q_+(f,f)(v) = \int\limits_{\mathbb{R}^3}\int\limits_{S^2} B(|u|,\mu) f\Big(v - \frac{1}{2}u + \frac{1}{2}|u|e\Big) f\Big(v - \frac{1}{2}u - \frac{1}{2}|u|e\Big)\,de\,du\,.$$

Switching to the spherical coordinates $u = r\,\tilde{e}\,,\ r > 0\,,\ \tilde{e}\in S^2$ leads to

$$\int\limits_0^\infty r^2 \int\limits_{S^2}\int\limits_{S^2} B(r,(e,\tilde{e})) f\Big(v - \frac{1}{2}r\,\tilde{e} + \frac{1}{2}r\,e\Big) f\Big(v - \frac{1}{2}r\,\tilde{e} - \frac{1}{2}r\,e\Big)\,de\,d\tilde{e}\,dr\,.$$

Forming the new variable $2\tilde{u} = r\,e\,,\ r^2 dr\,de = 8d\tilde{u}$ and immediately omitting the tilde signs over $\tilde{u}$ and $\tilde{e}$ we obtain

$$Q_+(f,f)(v) = 8\int\limits_{\mathbb{R}^3}\int\limits_{S^2} B(2|u|,\mu) f(v - |u|e + u) f(v - |u|e - u)\,de\,du\,. \tag{23}$$

Thus both post-collisional velocities now depend on the variable e in the same way. Now we remove this dependence from the expressions $v-|u|e+u$ and $v-|u|e-u$ using the Fourier transforms (19) and (20)

$$f(v-|u|e+u)f(v-|u|e-u)=\mathcal{F}_{y\to\xi}\Big[\mathcal{F}^{-1}_{z\to y}[f(z+u)f(z-u)](y)\Big]_{\xi=v-|u|e}.$$

Substituting this expression in (23) and using the integral form of the Fourier transform leads to

$$8\int\limits_{\mathbb{R}^3}\int\limits_{\mathbb{R}^3}\int\limits_{S^2} B(2|u|,\mu)e^{\imath(v-|u|e,\,y)}\mathcal{F}^{-1}_{z\to y}\Big[f(z+u)f(z-u)\Big](y)\,de\,du\,dy\,.$$

Thus together with the definition (22) we obtain the final result (21)

$$Q_+(f,f)(v)=\mathcal{F}_{y\to v}\Big[\int\limits_{\mathbb{R}^3} T(u,y)\mathcal{F}^{-1}_{z\to y}\Big[f(z-u)f(z+u)\Big](u,y)\,du\Big](v)\,.$$

■

Remark 2 *The expression (21) contains nine integrals instead of five in the original form (2). However no integration over the unit sphere is involved and two Fourier transforms in (21) can be evaluated very efficiently on the uniform grid using the algorithm of FFT.*

The kernel $T(u,y)$ defined in (22) does not depend on six variables. Even in the most general case of interaction (4) it depends only on $|u|$, $|y|$ and (u,y). To show this fact we rewrite (22) having the kernel (4) as follows

$$T(u,y)=2^{3+\lambda}|u|^\lambda\int\limits_{S^2} g_m\left(\frac{(u,e)}{|u|}\right)e^{-\imath|u|(y,\,e)}\,de\,,\ \lambda=1-4/m\,. \qquad (24)$$

Using the orthogonal matrix

$$U=\left(\frac{(u\times y)\times u}{|u\times y|\,|u|}\,\vdots\,\frac{u\times y}{|u\times y|}\,\vdots\,\frac{u}{|u|}\right)\in\mathbb{R}^{3\times 3}$$

we introduce the following parametrisation of the unit sphere

$$e=e(\varphi,\theta)=U\begin{pmatrix}\cos\varphi\,\sin\theta\\ \sin\varphi\,\sin\theta\\ \cos\theta\end{pmatrix}\,,\ 0\le\varphi<2\pi\,,\ 0\le\theta\le\pi\,.$$

Since

$$(u,e)=|u|\cos\theta\,,\ (y,e)=\frac{|u\times y|}{|u|}\cos\varphi\,\sin\theta+\frac{(u,y)}{|u|}\cos\theta$$

we obtain for the integral in (24) the following expression

$$\int_0^{\pi} g_m(\cos\theta) e^{-\imath(u,y)\cos\theta} \int_0^{2\pi} e^{-\imath|u\times y|\cos\varphi\,\sin\theta}\, d\varphi\, \sin\theta\, d\theta\,.$$

Using the Bessel function

$$J_0(z) = \frac{1}{2\pi}\int_0^{2\pi} e^{\imath z\,\cos\varphi}\, d\varphi$$

and the obvious formula

$$|u\times y| = \sqrt{|u|^2|y|^2 - (u,y)^2}$$

we obtain the following simplification

$$2\pi \int_0^{\pi} g_m(\cos\theta) e^{-\imath(u,y)\cos\theta} J_0\left(\sqrt{|u|^2|y|^2-(u,y)^2}\,\sin\theta\right)\sin\theta\, d\theta\,.$$

Thus

$$T(u,y) = T(|u|,|y|,(u,y))\,.$$

This property can be used for reducing the numerical work and/or the memory requirements.
For the VHS model of interaction (8) the function $T(u,y)$ can be computed analytically

$$T(u,y) = 2^{3+\lambda} C_\lambda |u|^\lambda \int_{S^2} e^{-\imath|u|(y,e)}\, de = 2^{5+\lambda}\pi C_\lambda |u|^\lambda \mathrm{sinc}(|u|\,|y|)\,,$$

where the abbreviation

$$\mathrm{sinc}z = \frac{\sin z}{z}\,,\ z\in\mathbb{R}$$

is used. In this case the kernel $T(u,y)$ depends only on two scalar values $|u|$ and $|y|$. This property will then help us to construct a more efficient scheme for the VHS model (8) than for the general model of interaction (4).

3 Discretisation of the collision integral

In this section we derive a discrete version of the Boltzmann collision integral

$$Q(f,f)(v) = Q_+(f,f)(v) - Q_-(f,f)(v)$$

with

$$Q_+(f,f)(v)\mathcal{F}_{y\to v}\Big[\int\limits_{\mathbb{R}^3} T(u,y)\mathcal{F}^{-1}_{z\to y}\Big[f(z-u)f(z+u)\Big](u,y)\,du\Big](v) \qquad (25)$$

and

$$Q_-(f,f)(v) = f(v)\int\limits_{\mathbb{R}^3} B_{tot}(|u|)f(w)\,dw\,, \qquad (26)$$

where the function $B_{tot}(|u|)$ is defined in (7).

3.1 Discretisation of the velocity space

The distribution function $f(t,v)$ is in general not compactly supported but usually it is negligibly small outside of some ball

$$B_L(V) = \left\{v \in \mathbb{R}^3 \,:\, |v-V| \le L\right\}\,,$$

where V denotes the bulk velocity (13). Thus for the numerical treatment of the Boltzmann equation we assume that

$$\operatorname{supp} f(t,\cdot) = B_L(V)\,,\ t \ge 0\,.$$

The support of the function

$$g^{(1)}(u,z) = f(z-u)f(z+u) \qquad (27)$$

with respect to the variable z by fixed u is the intersection of two balls and depends on u

$$\operatorname{supp} g^{(1)}(u,\cdot) = B_L(V-u)\bigcap B_L(V+u)\,.$$

It is clear that

$$\operatorname{supp} g^{(1)}(u,\cdot) = \emptyset\,,\ |u| > L\,.$$

The same property is obviously valid for the function

$$g^{(2)}(u,y) = \mathcal{F}^{-1}_{z\to y}\Big[g^{(1)}_u(z)\Big](y)\,, \tag{28}$$

with respect to the variable y i.e.

$$\operatorname{supp} g^{(2)}(u,\cdot) = \emptyset\,,\ |u| > L\,.$$

Thus the integration over the whole space $\mathbb{R}^3$ with respect to the variable u in (21) can be restricted to the ball $B_L(0)$. It is much more convenient to consider the cube

$$C_L(V) = \big\{v \in \mathbb{R}^3\ :\ |v_j - V_j| \le L\,,\ j = 1,2,3\big\}$$

instead of the ball $B_L(V) \subset C_L(V)$ for discretisation of the variables z, v and w in (25) and (26). $C_L(0)$ will be used for the variable u in (25).
Let $n \in \mathbb{N}$ be a natural even number. Then we denote by $C_n,\ C'_n$ the following sets of three-dimensional indices

$$\begin{aligned} C_n &= \big\{k \in \mathbb{Z}^3\,,\ -n/2 \le k_m \le n/2\,,\ m = 1,2,3\big\}\,, \\ C'_n &= \big\{k \in \mathbb{Z}^3\,,\ -n/2 < k_m \le n/2\,,\ m = 1,2,3\big\}\,. \end{aligned} \tag{29}$$

Introducing the mesh size $h_v = 2L/n$ in the velocity space we consider the following set of discrete velocities

$$C_v = \{v_j = V + h_v j\,,\ j \in C_n\} \subset C_L(V)\,. \tag{30}$$

The appropriate set for the variable u is

$$C_u = \{u_k = h_v k\,,\ k \in C_n\} \subset C_L(0)\,.$$

The variable y in (25) will be discretised on the set

$$C_y = \{y_j = h_y j\,,\ j \in C'_n\}\,, \tag{31}$$

where the mesh size h_y is related to the mesh size h_v by

$$h_v h_y = \frac{2\pi}{n}\,,\quad \text{i.e. } h_y = \frac{\pi}{L}\,. \tag{32}$$

3.2 Discretisation of the gain part (general case)

The computation of the gain part of the collision integral $Q_+(f,f)$ (25) consists of the computation of the integral of the function $g^{(2)}(u,y)$ (see (27),(28)) over $C_L(0)$ with respect to the variable u

$$g^{(3)}(y) = \int\limits_{C_L(0)} g^{(2)}(u,y)\, du$$

and of the final Fourier transform

$$Q_+(f,f)(v) = \mathcal{F}_{z\to y}[g^{(3)}(y)](v)$$

and can be realised using the following algorithm:

Algorithm 3

1. `Integration over` $C_L(0)$:

   `1.1 set` $g^{(3)}(y_j) := 0\,,\ \ y_j \in C_y\,,$

   `1.2 for all` $u_k \in C_u$ `compute`

   `1.2.1`

   $$g^{(1)}(u_k, z_l) := f(z_l - u_k) f(z_l + u_k)\,,\ \ z_l \in C_v\,,$$

   `1.2.2`

   $$g^{(2)}(u_k, y_j) := \frac{h_y^3}{(2\pi)^3} \sum_{z_l \in C_v} \omega_l\, e^{-\imath(y_j, z_l)} g^{(1)}(u_k, z_l)\,,\ \ y_j \in C_y\,,$$

   `1.2.3`

   $$g^{(3)}(y_j) := g^{(3)}(y_j) + \omega_k\, T(u_k, y_j)\, g^{(2)}(u_k, y_j)\,,$$

2. `Fourier transform:`

$$Q_+(f,f)(v_k) := h_y^3 \sum_{y_j \in C_y} \omega_j\, e^{\imath(v_k, y_j)} g^{(3)}(y_j)\,,\ \ v_k \in C_v\,.$$

Remark 4 *The values $\omega_k\,,\ k \in C_n$ in 1.2.2, 1.2.3 and 2. are the weights of a quadrature defined on the regular grids C_v, C_u and C_y. In our tests we will use the trapezoidal rule having the formal accuracy of $O(n^{-2})$ and which is very easy to implement. It should be pointed out that the use of more accurate quadrature rules such as the Simpson rule affect neither the amount of numerical work nor the practical realisation of the algorithm.*

Remark 5 `Step 1.2.1` *of the above algorithm can be realised very efficiently. Thus the pointwise multiplication is only necessary for the points* $z_l \in \operatorname{supp} g^{(1)}(u_k, \cdot)$. *Simple geometrical considerations show that the total number of multiplications required by this step is* $n^6/8 + O(n^5)$.

Remark 6 `Step 1.2.2` *is the most expensive in the whole algorithm. It can be written with (30), (31) and (32) in the form*

$$g^{(2)}(u_k, y_j) = \frac{1}{(2L)^3} e^{-\imath(y_j, V)} \sum_{l \in C'_n} \omega_l e^{-\imath \frac{2\pi}{n}(j,l)} g^{(1)}(u_k, z_l)\,.$$

Thus this step requires one FFT and one multiplication with the diagonal matrix

$$D = \operatorname{diag}\left\{ e^{-\imath(y_j, V)}\,,\ j \in C'_n \right\}$$

for every u_k *leading to* $15n^6 \log_2(n) + O(n^6)$ *complex multiplications.*

Remark 7 *The realisation of* `Step 1.2.3` *is obvious. If the values* $T(u_k, y_j)$ *can be precomputed and stored then the numerical work required by this step is exactly* $n^6 + O(n^5)$ *complex multiplications. We are going to discuss this procedure for the VHS model in the next section. If these values are computed in each time step then the numerical work required by* `Step 1.2.3` *remains of the same order* $O(n^6)$ *but having some probably unpleasant constant which will depend on the special choice of the kernel* $B(|u|, \mu)$.

Remark 8 *Final* `Step 2.` *of the algorithm reads as*

$$Q_+(v_k) = h_y^3 e^{\imath(v_k, V)} \sum_{j \in C'_n} \omega_j e^{\imath \frac{2\pi}{n}(k,j)} g^{(3)}(y_j)\,.$$

Thus this step requires one FFT and one multiplication with the diagonal matrix D^*. *The amount of numerical work* $15n^3 \log_2(n) + O(n^3)$ *is negligible in comparison with the previous steps.*

3.3 Discretisation of the gain part (VHS model)

The main advantage of the VHS model (8) is that the function $T(u, y)$ in (25) depends only on the values $|u|$ and $|y|$ (e.g. (25))

$$T(u, y) = 2^{5+\lambda} \pi C_\lambda |u|^\lambda \operatorname{sinc}(|u|\,|y|)\,.$$

Thus on the grid $C_u \times C_y$ we obtain with (32)

$$T(u_k, y_j) = T_{k,j} = 2^{5+\lambda}\pi C_\lambda h_v^\lambda |k|^\lambda \mathrm{sinc}\left(\frac{2\pi}{n}|k|\,|j|\right). \tag{33}$$

The matrix T contains many equal elements due to the following fact. The integer values $|k|^2$ and $|j|^2$ have the following range

$$0 \le |k|^2 \le \frac{3}{4}n^2\,,\ k \in C_n\,.$$

Thus the matrix T in (33) contains only $9/16n^4 + O(n^2)$ different values which can be stored in an array $\tilde{T}$ of the dimension $(3/4n^2+1)\times(3/4n^2+1)$. Then we use

$$T_{k,j} = \tilde{T}_{|k|^2,|j|^2}$$

for further calculations. The amount of computer memory is close to optimal but probably the main advantage of the VHS model is a remarkable reduction of numerical work due to the special form of the matrix T. In order to modify Algorithm 3 we divide the set C_n of all indices in classes of equivalence

$$C_n = \bigcup_{m=0}^{3/4n^2} Cl_m\,,\quad Cl_m = \left\{k \in \mathbb{Z}^3 \,:\, |k|^2 = m\right\}.$$

Note that due to the number theory there are no solutions $k \in \mathbb{Z}^3$ of the equation

$$k_1^2 + k_2^2 + k_3^2 = 7 \bmod 8\,.$$

Thus the corresponding classes $Cl_{7 \bmod 8}$ are empty. The following modification of Algorithm 3 is therefore possible:

Algorithm 9

1. `Integration over` $C_L(0)$:

   `1.1 set` $g^{(3)}(y_j) := 0\,,\ y_j \in Q_y\,,$

   `1.2 for all` $m = 0, 1, \ldots, 3/4n^2\,,\ m \neq 7 \bmod 8$ `compute`

   `1.2.1`

$$g^{(1)}(m, z_l) := \sum_{k \in Cl_m} \omega_k\, f(z_l - u_k) f(z_l + u_k)\,,\ z_l \in C_v\,,$$

`1.2.2`

$$g^{(2)}(m, y_j) := \frac{h_y^3}{(2\pi)^3} \sum_{z_l \in C_v} \omega_l \, e^{-\imath(y_j, z_l)} g^{(1)}(m, z_l) \,, \quad y_j \in C_y \,,$$

`1.2.3`

$$g^{(3)}(y_j) := g^{(3)}(y_j) + \tilde{T}_{m,|j|^2} \, g^{(2)}(m, y_j) \,,$$

`2. Fourier transform:`

$$Q_+(f,f)(v_k) := h_y^3 \sum_{y_j \in C_y} \omega_j \, e^{\imath(v_k, y_j)} g^{(3)}(y_j) \,, \quad v_k \in C_v \,.$$

Algorithms 3 and 9 are completely equivalent but Algorithm 9 is much faster. The main gain in efficiency is the reduction of FFT's in `Step 1.2.2` from $(n+1)^3$ in Algorithm 3 to $21/32n^2 + 1$ in Algorithm 9. Thus `Step 1.2.1` requiring $n^6/8$ multiplications is now asymptotically the most expensive step while all FFT's in `Step 1.2.2` require only $315/32n^5 \log_2(n)$ operations. However, `Step 1.2.2` is more expensive in practice than `Step 1.2.1` for realistic values of n.

3.4 The loss part of the collision integral

The computation of the loss part of the collision integral $Q_-(f,f)$ (26) consists of the computation of the linear integral operator of convolution type

$$g(v) = \int\limits_{C_L(V)} B_{tot}(|v-w|) f(w) \, dw \tag{34}$$

and of the pointwise multiplication of the functions $f(v)$ and $g(v)$ on the grid C_v. The discretisation of (34) leads to

$$g(v_k) = h_v^3 \sum_{w_j \in C_v} \omega_j B_{tot}(h_v|k-j|) f(w_j) \,.$$

Thus (34) describes a multiplication of the three-level Block-Toeplitz matrix having elements $h_v^3 B_{tot}(h_v|k-j|) \,, \; k,j \in C_n$ with the vector having elements $\omega_j f(w_j) \,, \; j \in C_n$. This standard task can be done numerically using $O(n^3 \ln(n))$ arithmetical operations with a rather unpleasant constant. However, this amount of work is negligible compared with the computation of the gain part. It is necessary to remark that the fast multiplication of a multilevel Block-Toeplitz matrix with a vector also requires some amount

of memory for the eigenvalues of the corresponding block-circulant matrix. This amount is $8n^3$ and in general quite important. Finally we compute

$$Q_-(f,f)(v_k) = f(v_k)g(v_k)\,,\ k \in C_n \tag{35}$$

using $O(n^3)$ multiplications. Note that for the Maxwell pseudo-molecules the function B_{tot} is constant and therefore the computation of the loss part is a trivial scaling

$$Q_-(f,f)(v_k) = \varrho_0 B_{tot} f(v_k)\,,\ k \in C_n\,. \tag{36}$$

3.5 Conservation properties

Here we follow [6] and describe the discrete version of the conservation properties (16), (17) and (18). For a given initial distribution $f_0(v)$ we first compute on the grid C_v the initial values

$$\begin{aligned}
\varrho_h &= h_v^3 \sum_{v_j \in C_v} \omega_j f_0(v_j)\,,\\
m_h &= h_v^3 \sum_{v_j \in C_v} \omega_j v_j\, f_0(v_j)\,,\\
M_h &= h_v^3 \sum_{v_j \in C_v} \omega_j |v_j|^2\, f_0(v_j)\,.
\end{aligned}$$

Then we introduce numerical conservation properties of the form

$$\begin{aligned}
h_v^3 \sum_{v_j \in C_v} \omega_j f(t,v_j) &= (f,\psi_0) = a_0\,, \qquad (37)\\
h_v^3 \sum_{v_j \in C_v} \omega_j (v_j)_l\, f(t,v_j) &= (f,\psi_l) = a_l\,,\ l = 1,2,3\,,\\
h_v^3 \sum_{v_j \in C_v} \omega_j |v_j|^2\, f(t,v_j) &= (f,\psi_2) = a_4\,,
\end{aligned}$$

where $(\cdot,\cdot) : \mathbb{R}^{(n+1)^3} \times \mathbb{R}^{(n+1)^3} \to \mathbb{R}$ is the Euclidean scalar product and $\psi_l \in \mathbb{R}^{(n+1)^3}$ are given vectors. Thus there are 5 algebraic constraints on the vector $f(t,\cdot)$ for all $t \geq 0$. In general they will not be fulfilled automatically and require some correction of the vector $f(t,\cdot)$ for $t > 0$. In [4], [5] and [6] we have developed and tested an effective algorithm for conservation properties (37) which is based on the Fourier transform. Here we give only a short summary of this algorithm and refer to the above articles for more details.

If

$$\hat{f}(t,\xi) = \int\limits_{\mathbb{R}^3} f(t,v) e^{\imath (v,\xi)} dv$$

denotes the Fourier transform of the distribution $f(t,v)$ then the conservation properties (16), (17) and (18) read as

$$\begin{aligned}
\int\limits_{\mathbb{R}^3} f(t,v)\, dv &= \hat{f}(t,\xi)|_{\xi=0}\,, \\
\int\limits_{\mathbb{R}^3} v\, f(t,v)\, dv &= -\imath\, \mathrm{grad}\hat{f}(t,\xi)|_{\xi=0}\,, \\
\int\limits_{\mathbb{R}^3} |v|^2\, f(t,v)\, dv &= -\Delta\hat{f}(t,\xi)|_{\xi=0}\,.
\end{aligned}$$

Thus for $\hat{f}$ everything is concentrated at zero. The conservation algorithm uses the property of the matrix of the discrete Fourier transform

$$F\,F^* = F^*\,F = n^3 I\,,\ f_{k,j} = e^{\imath \frac{2\pi}{n}(k,j)}\,,\ k,j \in C_n\,,$$

the analytical form (see [5]) of the discrete Fourier transforms of the vectors ψ_l in (37)

$$\hat{\psi}_l = F\,\psi_l\,,\ l = 0,\ldots,4$$

and equations (37) to obtain

$$(f,\psi_l) = \frac{1}{n^3}(\hat{f},\hat{\psi}_l) = a_l\,,\ l = 0,\ldots,4,. \tag{38}$$

Thus the whole procedure is simple. We compute the discrete Fourier transform of $f(t,\cdot)$ and obtain $\hat{f}(t,\cdot)$. Then we correct $\hat{f}(t,\cdot)$ in the points $(0,0,0)^T, (\pm 1,0,0)^T, (0,\pm 1,0)^T$ and $(0,0,\pm 1)^T$ corresponding to (38) and finally transform it back. The algorithm requires only $O(n^3 \ln(n))$ arithmetical operations. The numerical tests show that the correction is usually very small but important for the stability of the whole numerical procedure.

3.6 Time discretisation

After the discretisation of the Boltzmann collision integral the Boltzmann equation (1) is reduced to the initial value problem for the following system

of ordinary algebro-differential equations

$$\begin{aligned} \frac{df_k}{dt} &= Q_k(f,f)\,,\ f_k(0) = f_0(v_k)\,,\ k \in C_n\,, \\ (f,\psi_l) &= a_l\,,\ l = 0,\ldots,4\,. \end{aligned} \tag{39}$$

In (39) the collision integral is decomposed into the difference of $Q_+(f,f)$ which is computed corresponding to Algorithm 3 or Algorithm 9 and $Q_-(f,f)$ which is computed corresponding to (35) or (36). The simplest time discretisation of the system (39) is the Euler scheme

$$\begin{aligned} f^{(0)} &= \left\{f_0(v_k)\right\}_{k\in C_n}\,, \\ \tilde{f}^{(m+1)} &= f^{(m)} + \tau Q\left(f^{(m)}, f^{(m)}\right)\,, \\ f^{(m+1)} &= Conserve(\tilde{f}^{(m+1)})\,,\ m = 0,1,\ldots\,, \end{aligned}$$

where $\tau > 0$ is the time step and $Conserve$ denotes the conservation procedure described in the previous section. The formal accuracy of this discretisation is $O(\tau)$ which is, corresponding to our numerical tests, not sufficient compared with the accuracy of the discretisation of the collision integral which is $O(n^{-2})$. Since, in addition, the relaxation at the beginning is very fast, our numerical tests show that the error is dominated by $O(\tau)$ due to the time discretisation. Thus it is necessary to use a numerical scheme for the system (39) of at least second-order accuracy, for example the second-order Runge-Kutta scheme

$$\begin{aligned} f^{(0)} &= \left\{f_0(v_k)\right\}_{k\in C_n}\,, \\ f^{(m+1/2)} &= f^{(m)} + \frac{\tau}{2} Q\left(f^{(m)}, f^{(m)}\right)\,, \\ \tilde{f}^{(m+1)} &= f^{(m)} + \tau Q\left(f^{(m+1/2)}, f^{(m+1/2)}\right)\,, \\ f^{(m+1)} &= Conserve(\tilde{f}^{(m+1)})\,,\ m = 0,1,\ldots\,, \end{aligned}$$

which was perfect in all our tests.

4 Numerical examples

The careful check of new numerical methods requires a secure, possibly analytical solution of the problem. There are only few such solutions known. All of them are obtained for the Maxwell pseudo-molecules, one example being the famous BKW solution [2], [11]. However, the exact time evolution of the

moments (9)-(12) is available for an arbitrary initial distribution $f_0(v)$ (see [6]). If we assume that the collision kernel is constant

$$B(|u|,\mu) = \frac{1}{4\,\pi}$$

and the density is normalised $\varrho_0 = 1$ then the time evolution of the momentum flow and of the energy flow is given by

$$\begin{aligned} M(t) &= M(0)e^{-t/2} + (T_0\,I + V_0V_0^T)(1-e^{-t/2})\,; \\ r(t) &= r(0)e^{-t/3} + \frac{1}{2}(5T_0 + |V_0|^2)V_0(1-e^{-t/3}) \\ &+ (M(0) - V_0V_0^T - T_0\,I)V_0(e^{-t/2} - e^{-t/3})\,. \end{aligned}$$

Here V_0 and T_0 denote the conserved bulk velocity and the temperature. These values as well as the initial values $M(0), r(0)$ can be computed using the initial distribution $f_0(v)$.
As an example we consider the initial distribution $f_0(v)$ as a mixture of two different Maxwell distributions

$$f_0(v) = \alpha f_{M_1}(v) + (1-\alpha) f_{M_2}(v),\ 0 \le \alpha \le 1.$$

The parameters of the Maxwell distributions are V_1, T_1 and V_2, T_2. For the following simple but nontrivial choice

$$V_1 = (-2,2,0)^T,\ V_2 = (2,0,0)^T,\ T_1 = T_2 = 1,\ \alpha = 1/2$$

we obtain $T_0 = 8/3$ and

$$\begin{aligned} \varrho(t) &= \varrho_0 = 1\,; \\ V(t) &= V_0 = \begin{pmatrix} 0 \\ 1 \\ 0 \end{pmatrix}\,; \\ M(t) &= \begin{pmatrix} 5 & -2 & 0 \\ -2 & 3 & 0 \\ 0 & 0 & 1 \end{pmatrix} e^{-t/2} + \frac{1}{3}\begin{pmatrix} 8 & 0 & 0 \\ 0 & 11 & 0 \\ 0 & 0 & 8 \end{pmatrix}\left(1 - e^{-t/2}\right); \\ r(t) &= \frac{1}{2}\begin{pmatrix} -4 \\ 13 \\ 0 \end{pmatrix} e^{-t/3} + \frac{1}{6}\begin{pmatrix} 0 \\ 43 \\ 0 \end{pmatrix}\left(1 - e^{-t/3}\right) \\ &- \frac{1}{6}\begin{pmatrix} 12 \\ 4 \\ 0 \end{pmatrix}\left(e^{-t/2} - e^{-t/3}\right). \end{aligned} \tag{40}$$

The corresponding curves and their numerical approximations are presented in Figures 1,2 and 3.

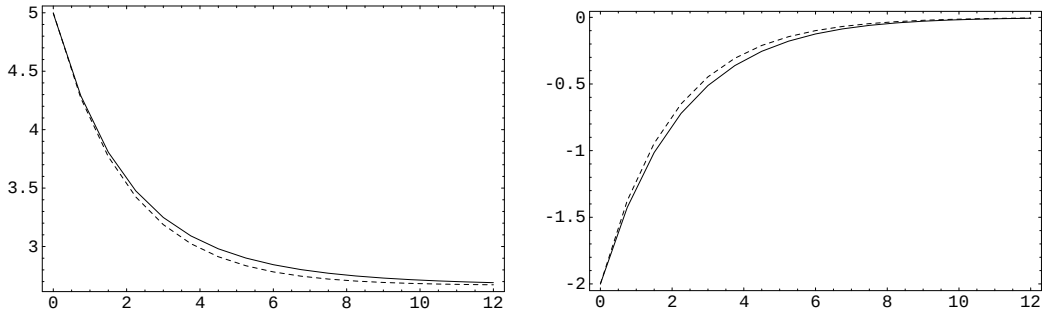

Figure 1. $M_{11}(t)$ and $M_{12}(t)$ and their approximations for $n = 8\,,\ M = 16$.

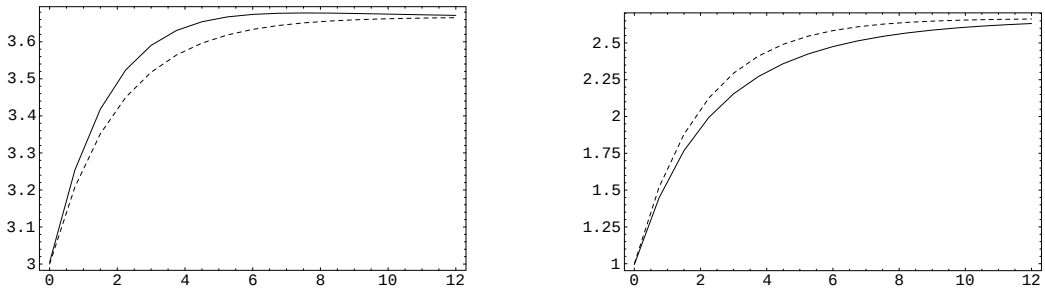

Figure 2. $M_{22}(t)$ and $M_{33}(t)$ and their approximations for $n = 8\,,\ M = 16$.

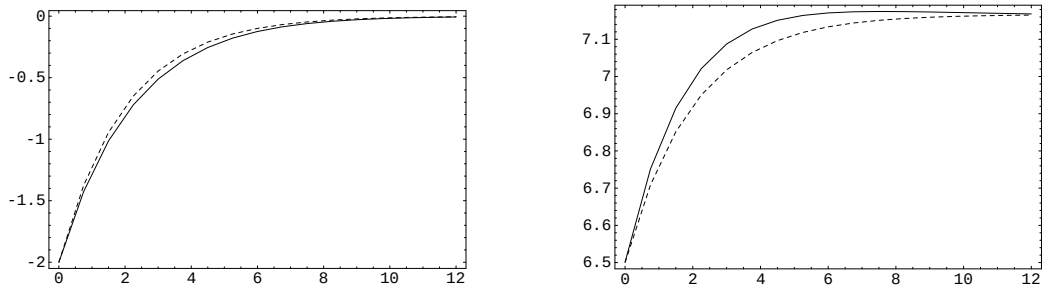

Figure 3. $r_1(t)$ and $r_2(t)$ and their approximations for $n = 8\,,\ M = 16$.

Here n denotes the number of discrete velocities in one direction (cf. (29)) and M is the number of time steps we used for discretisation of the time interval $[0, 12]$. Thus $\tau = 12/M$. The thick solid lines in the above figures represent the numerical solution while the thin dashed lines show the analytical curves. The quality of the numerical solution increases very quickly if we use more discretisation points. It is almost impossible to see any difference between the numerical and the analytical solution in a figure for $n \geq 12$, so we present the corresponding results in a form of tables.

n	M	$E_{max}(M_{11})$	$E_\infty(M_{11})$	CF	$E_{max}(M_{12})$	$E_\infty(M_{12})$	CF
8	16	0.678 E-01	0.182 E-01	-	0.714 E-01	0.171 E-01	-
16	32	0.466 E-02	0.168 E-03	14.5	0.519 E-02	0.206 E-03	13.8
32	64	0.135 E-02	0.548 E-04	3.5	0.116 E-02	0.470 E-04	4.5
64	128	0.326 E-03	0.132 E-04	4.2	0.279 E-03	0.113 E-04	4.2

Table 1. Numerical convergence of $M_{11}(t)$ and $M_{12}(t)$.

n	M	$E_{max}(M_{22})$	$E_\infty(M_{22})$	CF	$E_{max}(M_{33})$	$E_\infty(M_{33})$	CF
8	16	0.738 E-01	0.621 E-02	-	0.140 E-00	0.307 E-01	-
16	32	0.116 E-02	0.676 E-04	63.6	0.546 E-02	0.236 E-03	25.6
32	64	0.386 E-03	0.157 E-04	3.0	0.965 E-03	0.392 E-04	5.7
64	128	0.930 E-04	0.377 E-05	4.2	0.233 E-03	0.941 E-05	4.1

Table 2. Numerical convergence of $M_{22}(t)$ and $M_{33}(t)$.

n	M	$E_{max}(r_1)$	$E_\infty(r_1)$	CF	$E_{max}(r_2)$	$E_\infty(r_2)$	CF
8	16	0.142 E-00	0.342 E-02	-	0.142 E-00	0.631 E-02	-
16	32	0.104 E-01	0.411 E-03	13.7	0.232 E-02	0.135 E-03	61.2
32	64	0.231 E-02	0.939 E-04	4.5	0.771 E-03	0.313 E-04	3.0
64	128	0.558 E-03	0.226 E-04	4.1	0.186 E-03	0.753 E-05	4.1

Table 3. Numerical convergence of $r_1(t)$ and $r_2(t)$.

In the above tables n and M are as before. Tables 1-3 show the maximal error of the moments on the whole time interval as well as the final error computed as

$$E_{max}(q) = \max_{0\le m\le M} \left| q(t_m) - q_m \right|, \; E_\infty(q) = \left| q(t_M) - q_M \right|.$$

The convergence factor CF is the ratio of the maximal error in the given row and of the previous one. Thus we can see that the convergence is almost quadratic

$$E_{max} = O\Big(n^{-2} + M^{-2}\Big),$$

i.e. coincides with the quadratic convergence of the trapezoidal integration quadrature and second-order Runge-Kutta scheme used.
Using our new method we were able to solve the Boltzmann equation for $n = 96$ and $M = 192$ on a normal personal computer with 1.5GB memory. In the next table we present the results for M_{11} and M_{12}. The results for the other moments are very similar.

n	M	$E_{max}(M_{11})$	$E_{\infty}(M_{11})$	CF	$E_{max}(M_{12})$	$E_{\infty}(M_{12})$	CF
12	24	0.659 E-01	0.219 E-01	-	0.772 E-01	0.195 E-01	-
24	48	0.248 E-02	0.101 E-03	26.6	0.210 E-02	0.858 E-04	36.8
48	96	0.586 E-03	0.237 E-04	4.2	0.502 E-03	0.203 E-04	4.2
96	192	0.143 E-03	0.579 E-05	4.1	0.123 E-03	0.496 E-05	4.1

Table 4. Numerical convergence of $M_{11}(t)$ and $M_{12}(t)$.

The computational time for all examples is presented in the next table.

n	M	Time
8	16	6 sec
12	24	8 sec
16	32	24 sec
24	48	3 min
32	64	39 min
48	96	6 hours
64	128	45 hours
96	192	27 days

Table 5. Computational time for all examples.

We would like to point out that the parameters $n = 16$ and $M = 32$ already lead to high accuracy of all physical moments using very reasonable computational time. Thus we are now going to compare the numerical results obtained using this set of parameters with results obtained using the DSMC procedure for the Hard Spheres model (3). Note that in this case there is no analytical information about the moments.

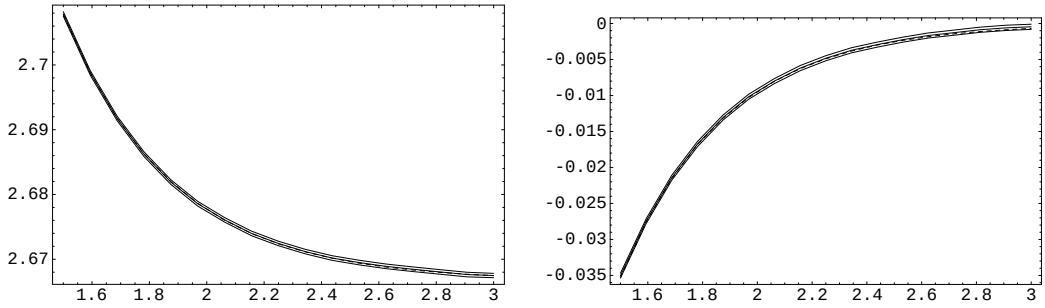

Figure 4. $M_{11}(t)$ and $M_{12}(t)$.

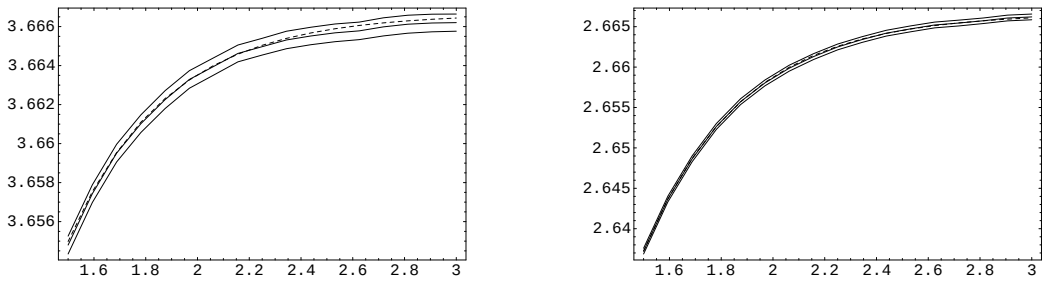

Figure 5. $M_{22}(t)$ and $M_{33}(t)$.

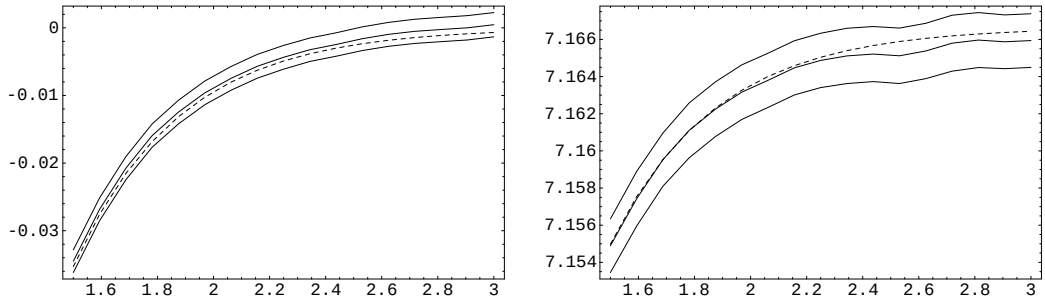

Figure 6. $r_1(t)$ and $r_2(t)$.

The pictures 4, 5 and 6 show the moments obtained using our new method (dashed lines), the empirical mean values obtained by the DSMC method with 10^6 particles and 1000 independent trajectories (thick solid line) as well as the corresponding confidence bands (thin solid lines) on the time interval $[1.5, 3.0]$. It can be seen that the agreement of the results is excellent. The difference (E_{max}) between the deterministic and stochastic numerical solutions is presented in Table 6.

$E_{max}(M_{11})$	$E_{max}(M_{12})$	$E_{max}(M_{22})$	$E_{max}(M_{33})$	$E_{max}(r_1)$	$E_{max}(r_2)$
0.628 E-03	0.858 E-03	0.538 E-03	0.964 E-03	0.209 E-02	0.190 E-02

Table 6. Difference between deterministic and stochastic solutions.

We remark that the DSMC solution took 17 hours computational time on the same personal computer while the deterministic solution was obtained within seconds.

Conclusions

In the present paper we develop a new deterministic numerical method for the Boltzmann equation. This method uses a special form of the gain part

of the Boltzmann collision operator which is available for all cut-off kernels and involves Fourier transforms. The discretisation uses a uniform grid in the velocity space, so the algorithm of Fast Fourier Transform can be applied to increase the efficiency of the method. Since no integration over the unit sphere is involved in the special form of the collision integral only simple numerical integration on a regular grid is applied, leading to a high degree of accuracy. This result forced us to use a second-order scheme for the time discretisation too in order to avoid any discrepancy in accuracy with respect to the velocity space and the time. The numerical results obtained are carefully tested using known analytical curves for the time relaxation of the moments for the Maxwell pseudo-molecules. The second-order accuracy of the method can be seen clearly. The comparisons with the DSMC results for the Hard Spheres model show very good agreement even for a relatively small number of discrete velocities and time steps. Further acceleration of the method presented can be achieved by replacing the numerical integration on the regular grid with respect to the variable u in (25) by some more efficient numerical integration procedure. At present we are thinking of employing the Gauß-Hermite quadratures for this integration. However, the main problem with using deterministic methods for the Boltzmann equation in a spatially non-homogeneous case occurs if the distribution function is not only significant in a small part of the velocity space covered by the cube C_v but has several different significant concentrations. In such situations it is still not clear whether deterministic schemes can compete with the DSMC.

References

[1] G. A. Bird. Monte Carlo simulation in an engineering context. *Progr. Astro. Aero*, 74 : 239–255, 1981.

[2] A. V. Bobylev. Fourier transform method in the theory of the Boltzmann equation for Maxwell molecules. *Doklady Akad. Nauk SSSR*, 225 : 1041–1044, 1975.

[3] A. V. Bobylev, A. Palczewski, and J. Schneider. On approximation of the Boltzmann equation by discrete velocity models. *C.R. Acad. Sci. Paris*, 320 : 639–644, 1995.

[4] A. V. Bobylev and S. Rjasanow. Difference scheme for the Boltzmann equation based on Fast Fourier Transform. *Eur. J. Mech. B/Fluids*, 16(2) : 293–306, 1997.

[5] A. V. Bobylev and S. Rjasanow. Fast deterministic method of solving the Boltzmann equation for hard spheres. *Eur. J. Mech. B/Fluids*, 18(5) : 869–887, 1999.

[6] A. V. Bobylev and S. Rjasanow. Numerical solution of the Boltzmann equation using fully conservative difference scheme based on the Fast Fourier Transform. *Transport Theory Statist. Phys.*, 29(3-5): 289–310, 2000.

[7] C. Cercignani, R. Illner, and M. Pulvirenti. *The Mathematical Theory of Dilute Gases*. Springer, New York, 1994.

[8] D. Goldstein, B. Sturtevant, and J. E. Broadwell. Investigation of the motion of discrete-velocity gases. In E.P. Muntz, D.P. Weaver, and D.H. Campbell, editors, *Rarefied Gas Dynamics: Theoretical and computational techniques*, pages 100–117. Progress in Astronomics and Aeronautics, 118, 1989.

[9] H. Grad. *Handbuch der Physik*, volume 12, pages 205–294. Springer-Verlag, Berlin-Göttingen-Heidelberg, 1958.

[10] S. Kosuge, K. Aoki, and S. Takata. Shock-wave structure for a binary gas mixture: Finite-difference analysis of the Boltzmann equation for hard-sphere molecules. *Eur. J. Mech., B/Fluids*, 20:87–, 2001.

[11] M. Krook and T.T. Wu. Exact solutions of Boltzmann equation. *Phys. Fluids*, 20(10), 1977.

[12] T. Ohwada. Structure of normal shock waves: direct numerical analysis of the Boltzmann equation for hard-sphere molecules. *Phys. Fluids A*, 5(1):217–234, 1993.

[13] T. Ohwada. Higher order approximation methods for the Boltzmann equation. *J. Comput. Phys.*, 139(1):1–14, 1998.

[14] A. Palczewski and J. Schneider. Existence, stability, and convergence of solutions of discrete velocity models to the Boltzmann equation. *J. Statist. Phys.*, 91(1-2):307–326, 1998.

[15] V. Panferov. Convergence of discrete-velocity models to the Boltzmann equation. Preprint 22, Chalmers University of Technology, Göteborg, 1997.

[16] V. A. Panferov and A. G. Heintz. A new consistent discrete-velocity model for the Boltzmann equation. *Math. Methods Appl. Sci.*, 25(7):571–593, 2002.

[17] L. Pareschi and B. Perthame. A Fourier spectral method for homogeneous Boltzmann equations. *Transport Theory Statist. Phys.*, 25 : 369–382, 1996.

[18] L. Pareschi and G. Russo. Numerical solution of the Boltzmann equation. I. Spectrally accurate approximation of the collision operator. *SIAM J. Numer. Anal.*, 37(4):1217–1245 (electronic), 2000.

[19] L. Pareschi and G. Russo. On the stability of spectral methods for the homogeneous Boltzmann equation. In *Proceedings of the Fifth International Workshop on Mathematical Aspects of Fluid and Plasma Dynamics (Maui, HI, 1998)*, volume 29, pages 431–447, 2000.

[20] F. Rogier and J. Schneider. A direct method for solving the Boltzmann equation. *Transport Theory Statist. Phys.*, 23(1-3) : 313–338, 1994.